


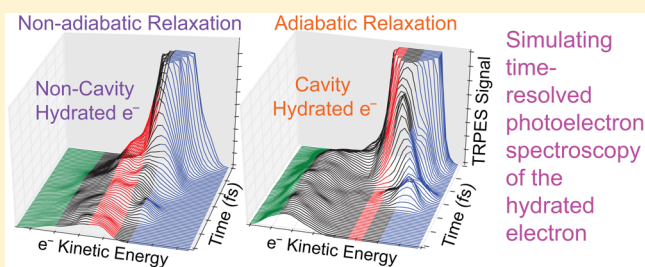
Time-Resolved Photoelectron Spectroscopy of the Hydrated Electron: Comparing Cavity and Noncavity Models to Experiment

Chen-Chen Zho and Benjamin J. Schwartz*

Department of Chemistry and Biochemistry University of California, Los Angeles, Los Angeles, California 90095-1569, United States

 Supporting Information

ABSTRACT: We use nonadiabatic mixed quantum/classical molecular dynamics to simulate recent time-resolved photoelectron spectroscopy (TRPES) experiments on the hydrated electron, and compare the results for both a cavity and a noncavity simulation model to experiment. We find that cavity-model hydrated electrons show an “adiabatic” relaxation mechanism, with ground-state cooling that is fast on the time scale of the internal conversion, a feature that is in contrast to the TRPES experiments. A noncavity hydrated electron model, however, displays a “nonadiabatic” relaxation mechanism, with rapid internal conversion followed by slower ground-state cooling, in good qualitative agreement with experiment. We also show that the experimentally observed early time red shift and loss of anisotropy of the excited-state TRPES peak are consistent with hydrated electron models with homogeneously broadened absorption spectra, but not with those with inhomogeneously broadened absorption spectra. Finally, we find that a decreasing photoionization cross section upon cooling causes the excited-state TRPES peak to decay faster than the underlying radiationless relaxation process, so that the experimentally observed 60–75 fs peak decay corresponds to an actual excited-state lifetime of the hydrated electron that is more likely ~100 fs.



INTRODUCTION

The hydrated electron, an excess electron in liquid water, is an important intermediate in charge-transfer reactions, photochemistry and radiation chemistry.^{1–4} As the simplest quantum mechanical solute, the hydrated electron system provides a perfect ground for the confrontation of experiment and simulation. Despite numerous papers discussing various properties of the hydrated electron, the physical structure of this object is still the subject of ongoing debate.^{4–13} Part of the issue is that despite its apparent simplicity, the hydrated electron is a tough object to tackle with traditional quantum chemistry techniques: the electron resides nearly entirely between the water molecules, and hundreds of waters in multiple configurations are needed to converge the calculated properties of this object. This is why much of the work in this field is still based on mixed quantum/classical simulations, where the water is treated classically, the excess electron quantum mechanically, and a pseudopotential is used to couple the classical and quantum degrees of freedom.

The conventional picture from mixed quantum/classical simulations is that due to Pauli exclusion-based repulsive interactions, the electron locally expels the water and resides in a cavity.^{14–17} Based on simulations with a new pseudopotential, however, we recently challenged this picture and suggested that many water molecules may reside inside the hydrated electron's wave function, giving a “noncavity” structure.^{5,18,19} Moreover, Uhlig et al. performed a series of DFT-based calculations and concluded that the hydrated electron has a “hybrid” structure with significant overlap of the electron's wave function with the

closest water molecules but also a small central cavity,²⁰ a picture supported by zero-K 4-water cluster continuum calculations.⁴ Although our potential⁵ has been the subject of controversy,^{6–8} largely because it does not do a good job predicting the vertical binding energies of water anion clusters,^{10–12} the noncavity structure it produces is more consistent with the hydrated electron's temperature-dependent properties and experimental resonance Raman spectrum¹⁸ as well as the electron's behavior near the air/water interface.^{21,22} We note, however, that the presence of interior waters packed at higher density than the bulk does not agree with the measured (positive) molar solvation volume of the electron.^{22,23}

Despite this controversy over the hydrated electron's physical structure, there is good consensus on its electronic structure, which is that of a quantum mechanical particle in a quasi-spherical box. For the cavity model, the electron is confined by the locally repulsive interactions of the surrounding solvent,^{16,17} whereas for the noncavity picture, the spherical box is comprised mostly of attractive polarization interactions from the interior water molecules.^{5,19} In either case, the hydrated electron has an “s-like” ground state and three quasi-degenerate “p-like” excited states. Within some small shifts, both cavity and noncavity models correctly predict the experimental absorption spectrum.^{5,16,17} Cavity models of the hydrated electron,

Received: August 3, 2016

Revised: November 12, 2016

Published: November 14, 2016

however, usually (but not always^{24,25}) predict that the absorption spectrum of the electron is inhomogeneously broadened,^{17,26,27} whereas both our noncavity model⁵ and experiments^{28–32} indicate that the electron's absorption spectrum is homogeneously broadened.

When photoexcited to one of its *p*-like excited states, the excited hydrated electron quickly relaxes back to its ground state via internal conversion. This process has been studied in pioneering work by Barbara and co-workers^{33–36} as well as in pump–probe transient absorption experiments by many other groups.^{31,37–39} The relaxation kinetics of the photoexcited hydrated electron is comprised of three distinct dynamical processes. First, the solvent rearranges to accommodate the structure of the excited electron, a process that raises the (unoccupied) ground-state energy of the electron.⁴⁰ Second, the excited electron undergoes a solvent-induced radiationless transition to the ground state. Finally, the newly created “hot” ground-state electron cools to return to equilibrium. Unfortunately, due to spectral overlap of the excited-state, hot ground-state and equilibrium ground-state absorption spectra, it is difficult to cleanly assign dynamical features of the transient absorption spectroscopy to each of these three processes. This has led to two models to explain the pump–probe transient absorption kinetics of the equilibrium hydrated electron. In the so-called “adiabatic” model, the hydrated electron occupies the excited *p*-like state for a relatively long amount of time (i.e., a few hundred fs), and then cools rapidly relative to the excited-state lifetime upon return to the ground state.^{26,40} In the “non-adiabatic” model, the electron returns quickly (i.e., in ≤ 100 fs) to the ground state, but the subsequent ground-state cooling is relatively slow, taking place on a hundreds-of-fs time scale.^{33,34}

This ambiguity over the excited-state relaxation dynamics of the hydrated electron has been largely resolved by the results of time-resolved photoelectron spectroscopy (TRPES) experiments, which were enabled by recent experimental advances in the development of vacuum liquid microjets.^{41–45} Neumark and co-workers lead the way by directly observing the binding energy of the electronic excited state, the decay of this excited state in ~ 75 fs, and the subsequent cooling of the hot ground state in ~ 410 fs, results that are strongly consistent with the nonadiabatic relaxation mechanism.^{46,47} More recent work by Suzuki and co-workers has revisited this problem using angle-resolved TRPES.⁴⁸ Their data showed a rapidly decaying anisotropy for the lower-energy peak, verifying its assignment to a *p*-like excited state, and a slightly shorter excited-state lifetime of ~ 60 fs and slightly longer ground-state cooling time of ~ 520 fs relative to that reported by Neumark and co-workers. These findings in support of the nonadiabatic relaxation mechanism are also consistent with pump–probe photoelectron spectroscopy studies on water cluster anions when the trend in excited-state lifetime with cluster size is extrapolated to the bulk.^{49–52}

Given that these time-resolved photoelectron spectroscopy experiments provide the cleanest examination of the photoexcited hydrated electron's relaxation dynamics, it is somewhat surprising that there has been essentially no effort made to directly connect the results of simulations to these experiments. Thus, in this paper, we simulate the time-resolved photoelectron spectroscopy experiment for both a cavity and a noncavity model of the hydrated electron. Our goals are to better understand the details of what this experiment measures and to determine which, if either, of the cavity and noncavity hydrated electron models is more consistent with experiment.

We find that the dynamics predicted by the noncavity model are in better qualitative agreement with experiment. In particular, the noncavity model is able to reproduce the experimentally observed early time red shift and loss of anisotropy of the excited-state TRPES peak, as well as the relatively slow ground-state cooling dynamics. The cavity model, in contrast, predicts little anisotropy loss for a blue-shifting excited-state peak, ground-state cooling that is faster than the excited-state lifetime, and a fairly large energy splitting between the excited-state and hot-ground-state TRPES peaks, none of which are seen experimentally. We also find that the cross sections for photoionization of the hydrated electron decrease between the excited *p*-like, hot ground and equilibrium ground states. The fact that the oscillator strength for photoionization decreases during the relaxation dynamics causes the experimentally measured decay of the *p*-state feature in the photoelectron spectrum to be faster than the actual underlying excited-state lifetime. Overall, our simulations clearly show that the experimental data are indeed consistent with the nonadiabatic relaxation mechanism, and suggest that the experimentally observed 60–75 fs decay corresponds to an underlying ~ 100 fs excited-state lifetime.

■ COMPUTATIONAL METHODS

Although we recognize that all-electron simulations would be preferred, we know of no computational methods for handling a system involving hundreds of water molecules plus an unpaired electron that resides between the molecule, particularly when the electron is promoted to one of a number of close-lying electronic excited states and then undergoes subsequent nonadiabatic relaxation. Thus, all of the simulations in this work consisted of one-electron mixed quantum/classical (MQC) molecular dynamics in the canonical (NVT) ensemble using in-house developed code; the methods we used are identical to those published in our previous hydrated electron work.^{5,13,18,19,21,53} Briefly, 499 flexible simple point charge (SPC-Flex)⁵⁴ water molecules were confined in a cubic simulation box of length 24.64 Å, ensuring a bulk water density of 0.997 g/cm³. The simulations used periodic boundary conditions, and the temperature of 298 K was enforced with a thermostat.⁵⁵

For the interaction between the quantum-mechanically treated hydrated electron and the classical water molecules, we chose to examine two different pseudopotentials derived from the Phillips-Kleinman formalism.^{56–58} We chose the potential developed by Turi and Borgis¹⁷ (TB) as a representative cavity hydrated electron model, and our more recent potential⁵ (referred to in the literature as LGS) as representative of the noncavity picture. As noted above, the LGS potential tends to overbind the electron,^{11,12} largely the result of the fact that it assumes condensed-phase charges for the water, which give a dipole moment $\sim 30\%$ larger than that of a gas-phase water molecule or a water molecule in a cluster.⁸ For clusters or bulk systems where the electron resides in a cavity or at the surface and is thus far from the water molecules, the TB potential does reasonably well with binding energies, but we have shown recently that this is only because of a fortuitous cancellation of errors between the static exchange and polarization terms in the potential.¹³ When the electron is confined to be closer to the water, as would be the case for a hybrid or noncavity structure, the TB model significantly underbinds compared to quantum chemistry calculations at both the MP2 and CCSD(T) levels. When we correct the ad

hoc polarization term in the TB potential to match the binding energies with CCSD(T) calculations at both short and long-range, we find that the resulting modified pseudopotential yields a noncavity electron whose behavior is similar to that of the LGS model.¹³

Thus, neither of the pseudopotentials we use are able to reproduce binding energetics for a variety of electron-water geometries, particularly those with interior waters. However, because we are limited to one-electron simulations for computational reasons, we thought it was best to choose potentials whose behavior and properties are well characterized in the literature.^{5,10,17–19,21,22} Thus, for the purposes of this work we treat each of the two potentials as ad hoc; we see these potentials as a means to produce hydrated electrons at the limits of cavity and noncavity structures, but expect neither to fully reproduce all possible properties of the hydrated electron. It would be quite interesting to see how well the DFT-based many-electron hybrid model of Uhlig et al.²⁰ would do in predicting the results of the TRPES experiments considered here, but unfortunately, given the need for excited states and electronically nonadiabatic dynamics, this remains beyond the scope of this work.

Once we had the desired potential implemented, we solved Schrödinger's equation using a $16 \times 16 \times 16$ grid basis set for the TB cavity electron, and a $32 \times 32 \times 32$ grid basis for the LGS noncavity electron, as needed to guarantee conservation of energy to better than 0.01 eV for the mixed quantum/classical systems during both equilibrium and nonequilibrium simulations. The quantum force exerted on the water molecules by the excess electron was calculated via the Hellmann–Feynman theorem, and the classical particles' dynamics were propagated using the velocity Verlet algorithm. We chose to use a cutoff for the electrostatic interactions at half the box length instead of Ewald summation both because Ewald summation is known to give a stronger finite size effect for this system^{10,21,22} and to be consistent with our previously published work.^{5,18,19,21}

After running a 200 ps equilibrium trajectory with each of our chosen pseudopotentials, we then simulated the dynamics following photoexcitation with 50 nonequilibrium trajectories promoting ground-state electron configurations to one of the adiabatic excited states. We selected excitation wavelengths for the cavity and noncavity models (1.73 ± 0.05 eV for TB and 1.59 ± 0.05 eV for LGS) to match the average energy gap between the ground state and lowest *p*-like excited state, and we chose uncorrelated configurations to start the nonequilibrium trajectories where any one of the hydrated electron's energy gaps fell within this energy range. This meant that for the inhomogeneously broadened absorption spectrum predicted by the TB model, most of the nonequilibrium trajectories were excited to the lowest or second-lowest *p*-like excited state. In contrast, for the homogeneously broadened absorption spectrum predicted by the LGS model, the hydrated electron was promoted to even higher-lying excited states 33% of the time (see the [Supporting Information \(SI\)](#)). We note that the nonequilibrium results obtained for the LGS hydrated electron are in agreement with those published in our earlier work;⁵ as far as we are aware, these are the first nonadiabatic excited-state trajectories ever run with the TB model.

To account for the breakdown of the Born–Oppenheimer approximation and propagate electronically nonadiabatic dynamics, we used Tully's fewest switches surface hopping (FSSH) algorithm⁵⁹ for each of our 50-member nonequilibrium

ensembles. It is important to note, however, that the FSSH algorithm does not provide a realistic picture of the decoherence that induces surface hopping for strongly coupled systems such as the hydrated electron. This is because FSSH technically requires that a swarm of trajectories be run from each classical initial condition, with the trajectories in that swarm added at the amplitude level in order to damp coherence.⁶⁰ Since it is impractical to add many nonadiabatic hydrated electron trajectories at the amplitude level, we are left with an improper estimate of the decoherence time. Moreover, the nonadiabatic transition rate of the hydrated electron depends sensitively on the decoherence time.^{53,61–63} This means that the excited-state lifetimes calculated in nonequilibrium trajectories (even if the trajectories were run with a many-electron level of theory rather than with a pseudopotential) will at best be estimates of the true lifetime. Thus, caution is recommended before attempting any type of direct quantitative comparison of calculated lifetimes using FSSH to experiment.

In previous work, we developed an expression to estimate the decoherence time in mixed quantum/classical simulations that was based on how the motions of Frozen Gaussian wave functions representing the classical nuclei diverge on different adiabatic potential energy surfaces.^{61,64} When we use this expression, we find that the decoherence time of the TB hydrated electron is less than half that of the LGS electron; see the [SI](#). Since the nonadiabatic transition rate varies in the same direction as the decoherence time⁶¹ and since FSSH gives roughly similar lifetimes for the two different hydrated electron models, this suggests that the LGS electron would have a significantly shorter calculated excited-state lifetime than the TB electron if decoherence were properly accounted for. Thus, even though both the TB and LGS hydrated electrons show simulated lifetimes with FSSH that are longer than those seen in experiment, the lifetimes for both models are in the correct ballpark relative to both experiment^{46,48} and to theoretical estimates based on Fermi's golden rule.⁶⁵ Thus, our simulations are still able to provide a good test of whether the adiabatic or nonadiabatic relaxation picture is more consistent with the pump–probe photoelectron experiments.

Finally, to predict the results of TRPES experiments from our simulations, we began with the straightforward assumption that the electron binding energy is equal to the calculated quantum energy in the simulation. The LGS model is known to overbind the electron,^{5,6,8} but for any hydrated electron model, the overall binding energy can be tuned by several eV simply by adjusting the pairwise-additive term in the pseudopotential that represents the electronic polarization of the classical water by the electron. Thus, our focus in this work is on the observed photoelectron spectroscopy dynamics, rather than the absolute binding energies. To calculate how the electron binding energy changes with time, we first histogrammed the electronic energy levels of the relaxing hydrated electrons in our simulated nonequilibrium ensembles into 0.1 eV width bins. We then weighted each configuration by ionization cross sections calculated as the square of the transition dipoles between the occupied electronic state and that of a free (plane wave) electron with an energy equal to the difference between the ionization photon energy and the electron binding energy. The ionizing (probe) photon energies, 5.0 eV for the TB model and 7.0 eV for LGS, were chosen so that the detached electron's kinetic energy for both models fell in the same energy range as in the experiments by Neumark and co-workers.⁴⁶ The details

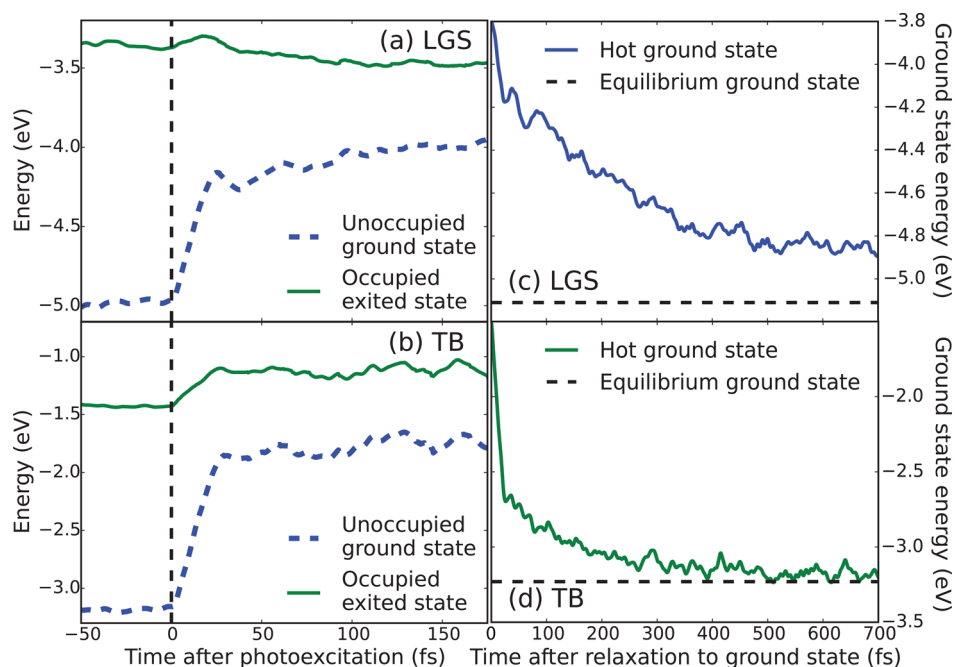


Figure 1. Nonequilibrium behavior of different models of the photoexcited hydrated electron. Nonequilibrium averages over the 50-member ensembles while an excited-state is occupied are shown for (a) the LGS and (b) the TB models. Dynamical history of the adiabatic ground-state energy level of the hydrated electron during ground-state cooling are shown for (c) LGS noncavity and (d) TB cavity models. Time zero for (a) and (b) was chosen to be the moment of photoexcitation, and for (c) and (d) the zero of time is chosen as the time step when the electron undergoes nonadiabatic relaxation to the ground state. The black dashed horizontal lines in (c) and (d) mark the equilibrated ground-state energy for each model. The data make clear that the LGS electron follows the “nonadiabatic” relaxation picture while the TB electron’s dynamics is more consistent with the “adiabatic” relaxation picture. The ground-state cooling time of the LGS electron is in good agreement with that seen experimentally.^{46,48}

of how we calculated the ionization cross sections are given in the SI. We also convoluted the data with an 80 fs fwhm Gaussian along the time axis to best model the experimental instrument response. The experiments by Suzuki and co-workers were reported only after we had completed our trajectories,⁴⁸ so when comparing to these experiments, which used a lower-energy photon for photoionization than the experiments by Neumark and co-workers, we simply shifted the energy axis of our calculated raw TRPES signals by 1.5 eV (for LGS) and 0.8 eV (for TB). In the SI, we show that the relative photoionization cross sections do not change significantly for different choices of the photoionization wavelength, so that a simple shift of the energy axis is indeed sufficient to best compare our calculations to experiments using different ionization photon energies.

RESULTS AND DISCUSSION

Cavity and Noncavity Hydrated Electrons Show Adiabatic and Nonadiabatic Relaxation Mechanisms, Respectively. We begin our discussion by comparing the excited-state relaxation dynamics of a cavity (TB)¹⁷ and a noncavity (LGS)⁵ model of the hydrated electron. Figure 1, panels a (LGS noncavity model) and b (TB cavity model), show the nonequilibrium ensemble average of the ground- (blue dashed curves) and excited-state (green solid curves) energy levels while the hydrated electron occupies an excited state; representative individual trajectories are given in the SI. For both hydrated electron models, following simulated photoexcitation at time zero, solvent motions cause the energy of the unoccupied ground state to increase dramatically, closing the energy gap.

During the first few tens of fs after excitation the average excited-state energy of the LGS noncavity electron drops slightly (~ 100 meV), primarily due to radiationless relaxation among different excited states (excitation to the lowest excited-state leaves the p -state energy unchanged, as we have documented previously⁵). The TB cavity electron, in contrast, shows a rapid (≤ 50 fs) ~ 300 meV increase in the occupied excited-state energy due to solvent motions that destabilize the p -like excited states. This rapid increase appears to be unique to the TB model, as previous studies of alternate cavity-model hydrated electrons found little change in the occupied p -state energy following photoexcitation.²⁷ This predicted difference in early time behavior between the LGS and TB hydrated electron models should be observable by time-resolved photoelectron spectroscopy, as discussed further below. It is worth noting that with our 50-member nonequilibrium ensembles, the average eigenenergies do not appear smooth; this is because 50 trajectories is insufficient to average over the phase of low-frequency librational and translational water motions that are displaced upon excitation, leaving some “ringing” at the displaced solvent frequencies.⁴⁰

The closing of the energy gap following excitation seen in Figure 1a and b is what allows the hydrated electron to undergo internal conversion to the ground state. The simulations predict a survival probability for the electron to remain in the excited state of a few hundred fs (see the SI), but as discussed above in the Computational Methods, the absolute value of the hydrated electron’s calculated excited-state lifetime is not terribly meaningful because of the limitations in the way the nonadiabatic surface-hopping algorithm treats decoherence. Moreover, as noted in the SI, if we had a better treatment of decoherence, we would expect the more coherent LGS model

to have a shorter excited-state lifetime than the less coherent TB model. The fact that the calculated lifetimes for both models are in the range of 100–300 fs, however, provides enough qualitative agreement with experiment to ensure that there is meaning in the dynamics underlying the calculated TRPES signals from these simulations.

Because the ground-state energy of the hydrated electron rises by hundreds of meV in the first ~ 40 fs following photoexcitation, even if the lifetime of the hydrated electron is only 60 to 75 fs,^{46,48} the newly created ground-state electrons produced by internal conversion must be out of equilibrium. To better visualize the “cooling” of the “hot” ground-state electrons, panels c (LGS) and d (TB) of Figure 1 show the dynamics of the nonequilibrium-ensemble-averaged ground- and excited-state adiabatic energy levels, where the average starts at the time of the nonadiabatic transition to the ground state for each of the 50 trajectories. For the TB cavity model, nearly 70% of the ground-state cooling takes place in the first ~ 40 fs after internal conversion, and the remaining cooling is essentially entirely complete within 300 fs (with a roughly exponential decay time for the slower cooling component of ~ 130 fs). In contrast, for the LGS noncavity electron, only $\sim 30\%$ of the cooling takes place at early times and the bulk of the ground-state cooling is not fully complete for over 1 ps, with a roughly exponential decay time of ~ 450 fs for the slow component, in excellent agreement with experiment.^{46,48}

The contrast between the cooling of the TB and LGS hydrated electrons is large enough that we can make definite statements in terms of the “adiabatic” and “nonadiabatic” relaxation pictures discussed in the Introduction, even without a direct simulation handle of the absolute numerical value of the excited-state lifetime. The TB cavity electron clearly follows the adiabatic relaxation picture, with ground-state cooling that is fast compared to the excited-state lifetime (even if the lifetime is under 100 fs), whereas the LGS noncavity hydrated electron shows large-amplitude ground-state cooling that is significantly slower than any reasonable excited-state lifetime, falling squarely into the nonadiabatic relaxation picture.

The fact that cavity and noncavity hydrated electrons follow separate adiabatic and nonadiabatic relaxation mechanisms makes sense given the structures associated with each model. For cavity electrons, the nonadiabatic relaxation mechanism involves removal of the node of the *p*-like excited-state, which resides in a roughly peanut-shaped cavity. The node is removed by collapse of the wave function into a single lobe of the peanut-shaped excited-state cavity.⁴⁰ The water molecules surrounding both lobes of the peanut are already well-oriented to solvate a newly created single-lobe ground-state electron. Thus, after collapse to the ground state, inertial motions of just a few surrounding water molecules are sufficient to complete the bulk of the subsequent cooling,^{40,66} explaining why the return to equilibrium after the nonadiabatic transition is so fast for the TB model. Thus, for TB, the more rapid closing of the energy gap after internal conversion compared to that after photoexcitation represents a breakdown of linear response due to the change in effectiveness of the inertial librational solvent motions associated with the different ground and excited-state cavity structures.⁶⁷ In contrast, the noncavity LGS hydrated electron contains many interior water molecules in both the ground and electronic excited states. When the *p*-like excited state undergoes internal conversion, both the local structure and density of the water molecules are poorly positioned to solvate the newly created *s*-like ground state, requiring relatively

slow diffusive orientational and translational motions of the interior waters to re-establish equilibrium, and leading to a less severe breakdown of linear response.

Simulated TRPES of Cavity and Noncavity Hydrated Electrons. With the nonequilibrium ensembles for the TB and LGS electrons in hand, we now turn to calculations of the time-resolved photoelectron spectroscopy for both electron models to provide a direct comparison with experiment. The simulated transient photoelectron spectra calculated from the nonequilibrium trajectories for both the cavity and noncavity hydrated electrons are shown as color contour plots in Figure 2a and b, with the experimental data from Suzuki and co-workers shown in Figure 2c.⁴⁸ The simulated data are also displayed as surface plots in the SI and the TOC graphic, along with the spectral windows used to examine the calculated kinetics of the equilibrium ground, hot ground and excited states of the hydrated electron shown below in Figure 4. Both simulated hydrated electrons show the immediate appearance of a peak due to occupation of the *p*-like excited state at higher kinetic energies, which rapidly decays into a peak at lower kinetic energies that corresponds to the *s*-like ground state. As mentioned above, the absolute value of the calculated electron kinetic energy along the *x*-axis of Figure 2 is not significant as the electron binding energy for both potentials is not terribly accurate, particularly when there are interior waters present, and can be tuned over a large range by making subtle changes in the polarization term in the electron-water pseudopotentials.¹³ Given that both models do a good job of reproducing the experimental absorption spectrum, however, we expect that the relative energies between the observed peaks and their dynamics should be meaningful.

One of the most obvious features of the data for both models in Figure 2, like that seen experimentally, is that the high-kinetic-energy peak corresponding to ionization of the *p*-like excited state has a higher amplitude than the lower-kinetic-energy peak corresponding to the ground state. This is because the cross sections for ionization from the different states are quite different, as summarized in Table 1. In general, we see that the excited states of the hydrated electron have larger transition dipole moments with an outgoing plane wave than does the ground state. This, along with the Jacobian factor for collecting low-kinetic-energy electrons, explains why the recovering ground-state dynamics are more difficult to resolve in the experiment than the excited-state dynamics.^{46,48} In the SI, we also show that the cross-section for ionization of the ground state is strongly correlated with the electron's binding energy: the “hotter” the ground-state electron, the larger the ionization cross-section. Thus, the photoionization cross-section of the ground-state hydrated electron decreases as the electron cools. This tends to exaggerate the cooling dynamics of the electron in the photoelectron spectroscopy, which somewhat compensates for the overall lower oscillator strength and Jacobian factor that leads to generally poorer signal-to-noise.

It is important to note that the true experimental TRPES cross-section also depends on factors such as the inelastic scattering of the ionized electrons with the water molecules encountered prior to escaping into the vacuum, which in turn depends on the shape of the electron's wave function and the depth at which the electron resides relative to the surface. Since the exact probing depth of TRPES is not well understood, we consider modeling these effects to be beyond the scope of this paper. The cross sections we calculate for the *p*-like excited

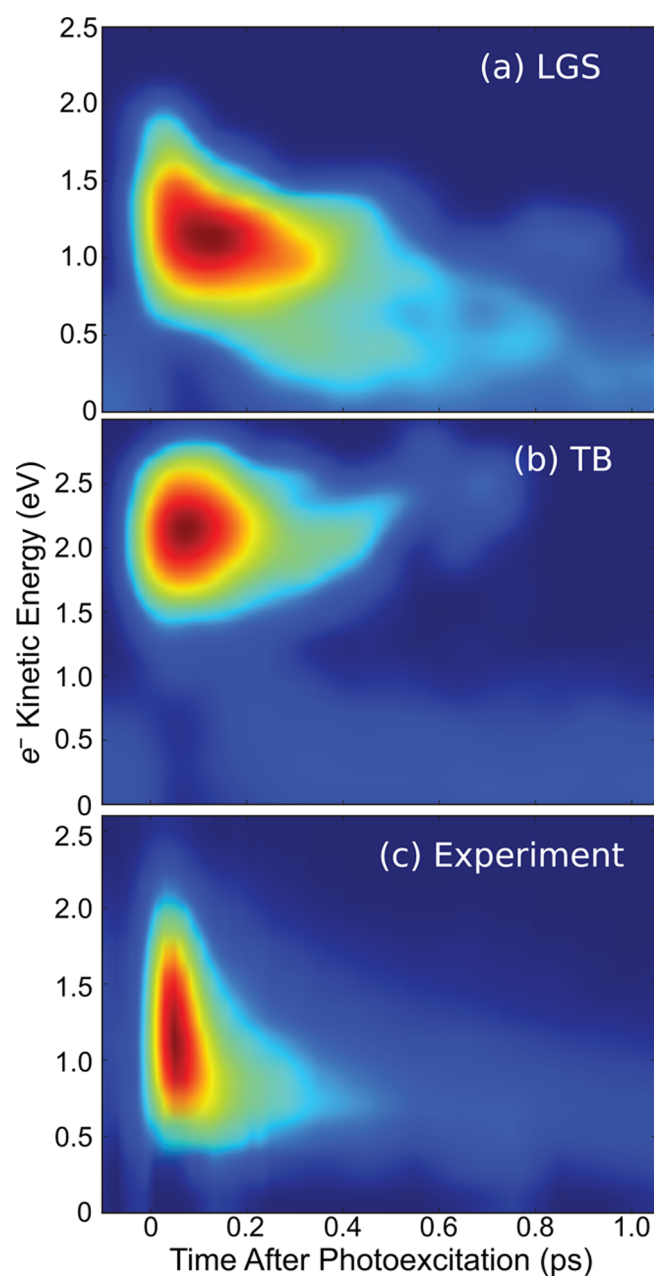


Figure 2. Calculated TRPES signals for the (a) LGS and (b) TB models of the hydrated electron (to be compared directly to the experimental data of Suzuki and co-workers,⁴⁸ reproduced in panel (c)); the magnitude of the TRPES signal decreases from red (highest signal intensity) to dark blue (zero signal) in spectral order. For both simulation models and the experiment, the higher-kinetic-energy peak corresponds to ionization from the *p*-like excited state, and the lower-kinetic-energy peak corresponds to the recovered *s*-like ground state. The LGS signal clearly shows the cooling of the hot ground state, consistent with the “nonadiabatic” relaxation picture and the experiments of refs 46 and 48. The TB data, in contrast, shows essentially two-state kinetics (i.e., *p*-state decaying directly into an essentially equilibrated *s*-state) that is representative of the “adiabatic” relaxation picture, which is not seen experimentally.

states relative to the ground state are indeed larger than what is seen experimentally, which suggests that the ground and excited state hydrated electrons either have different inelastic scattering or different average depths from the surface.⁴⁸ It is worth noting, however, that for both the TB and LGS models,

Table 1. Average Photoionization Cross Sections for Different *p*-like Excited States and Both the Hot and Equilibrated *s*-like Ground States for Cavity and Noncavity Models of the Hydrated Electron^a

e ⁻ model	third <i>p</i> -like state	second <i>p</i> -like state	lowest <i>p</i> -like state	“hot” ground state	eqb. ground state
LGS	12 ± 5	10 ± 4	7 ± 2	1.8 ± 0.3	1.0 ± 0.1
TB		19 ± 5	21 ± 6	7 ± 1	1.0 ± 0.3

^aThe cross section to ionize the equilibrium ground state is normalized to unity for each of the two hydrated electron models. The *p*-like excited states have higher cross sections than the ground state, explaining the stronger signals for this peak. The fact that internal conversion between *p*-like excited states (following excitation of a hydrated electron with a homogeneously-broadened absorption spectrum) leads to a dynamic reduction in ionization oscillator strength causes the *p*-state peak to decay more quickly than the underlying excited-state lifetime, as discussed in the text.

electrons within 1 nm of the water surface show completely bulklike properties,²² justifying our neglect of the surface in these simulations

When comparing each of the two hydrated electron models’ calculated TRPES signal to experiment, it is important to remember that because of how decoherence is treated in the surface-hopping algorithm we use, the simulated excited-state lifetimes are ~200 fs. This is longer than that observed experimentally, so the calculated TRPES signals seen in Figure 2 also persist to longer times than those seen experimentally. But, other than the more persistent dynamics, we see excellent agreement between the experimental signal and the simulated dynamics in Figure 2a. After the loss of the initially created *p*-like excited state, we see clear signatures of cooling of the hot LGS electron’s ground state produced after internal conversion, with a readily evident dynamic shift of the peak to lower kinetic energies. This is a direct reflection of the slow, “nonadiabatic”-picture relaxation of the ground state seen in Figure 1c, and is in accord with experiment.^{46,48} In contrast, Figure 2b shows almost no shifting of the TB electron’s ground-state peak with time, as expected from the rapid “adiabatic”-picture ground-state recovery seen in Figure 1d. The TB electron’s TRPES signal also shows two-state kinetic character that is in contrast to experiment, with the disappearance of the *p*-like state directly producing the equilibrated *s*-like state with a loss of ~1.5 eV of energy. Thus, our calculations indicate that the experiments are indeed consistent with the “nonadiabatic” relaxation picture of the hydrated electron, and that the LGS noncavity model better captures the experimentally observed features than the TB cavity model.

To examine the predicted TRPES of the two electron models in more detail, in Figure 3, we plot the instantaneous photoelectron spectrum of the *p*-like excited state for each model and for experiment at early times, with the amplitudes at each time normalized to better see the shapes and positions of the peaks. For the TB cavity model, panel b shows that the *p*-like excited-state peak shifts to higher kinetic energy and narrows during the first few tens of fs following photoexcitation, reflecting the rapid rise of the occupied *p*-state’s energy seen in Figure 1b. This shift to higher energies is opposite to what is seen in early times by experiment, as shown in the TRPES data from the Suzuki group in Figure 1c.⁴⁸ In contrast, Figure 3a shows that the position of the *p*-like excited-state peak of the LGS noncavity model shifts slightly to lower

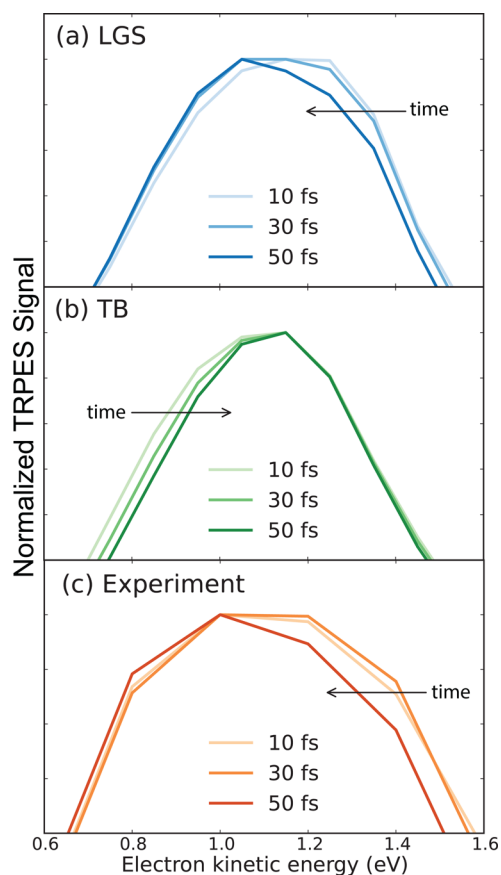


Figure 3. Normalized time slices of the early time calculated TRPES signals for the photoexcited (a) LGS noncavity and (b) TB cavity hydrated electrons and (c) the experimentally measured data,⁴⁸ same data as in Figure 2. The time goes from 10 to 50 fs as the thickness of the plotted lines increases and the color darkens. The early time shift to lower kinetic energies seen in (a) agrees well with the experiments of ref 48. in (c), whereas the narrowing and shift to higher kinetic energies in (b) stands in contrast to experiment.

kinetic energies over this same time period (cf. Figure 1a), in much better agreement with the experimental data shown in Figure 3c.⁴⁸ This is a direct result of the homogeneous broadening of the absorption spectrum of the LGS model of the hydrated electron, which means that photoexcitation populates a wide variety of excited states (see below). The rapid internal conversion between these excited states is what causes the experimentally observed shift to lower kinetic energy at early times.

To make contact with experiment in yet another way, we have integrated the calculated transient photoelectron signals over three different energy regions that correspond to the three “lanes” used in the analysis of the experimental data taken by Neumark and co-workers (cf. Figure 4 of ref 46 and see the SI for details). The results of this procedure are shown in Figure 4, with the blue dashed curves showing the *p*-state region, the red dotted curves denoting the high kinetic-energy side of the ground state, and the green solid curves representing the recovered equilibrium ground state for the LGS (panel a) and TB (panel b) models, and experiment (panel c).⁴⁶ The integration windows for the *p*-state region were 0.0–1.1 eV for LGS, 0.0–0.8 eV for TB, and 0.6–1.2 for the experiments; those for the hot ground state were 2.0–2.5 eV for LGS, 2.3–2.7 eV for TB, and 1.7–2.1 eV for the experiments; and those

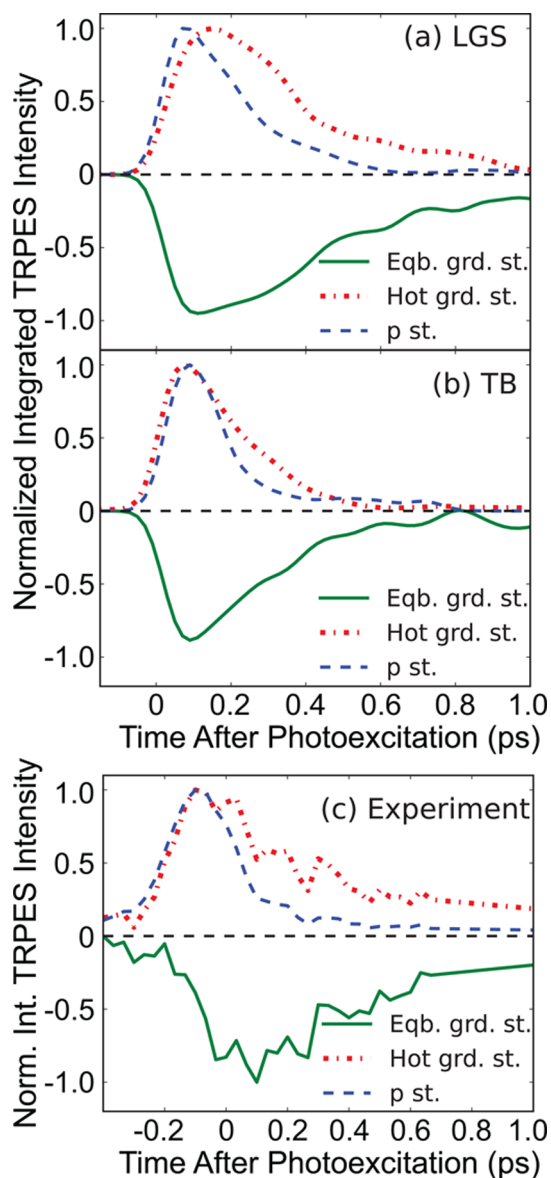


Figure 4. Kinetics of the pump–probe photoelectron spectroscopy integrated over various energy windows for the (a) LGS noncavity and (b) TB cavity models of the hydrated electron, and (c) the experimental data of Neumark and co-workers.⁴⁶ With ionization energies chosen to best match the experimental conditions of ref 46., the blue dashed curves show integration over 0–1.1 eV for LGS, 0–0.8 eV for TB and 0.6–1.2 eV for the experiments, corresponding to the *p*-like excited state; the red dotted curve is for integration over 2.0–2.5 eV for LGS, 2.3–2.7 eV for TB and 1.7–2.1 eV for the experiments, corresponding to the high-energy “hot” side of the *s*-like ground state; the green solid curve is for integration from 2.5 to 3.8 eV for LGS, 3.0–4.0 eV for TB, and 2.5–2.9 eV for the experiments, corresponding to the equilibrium ground state. The fact that the equilibrium ground-state recovery is much longer than the excited-state decay for LGS and experiment is a clear signature of the “nonadiabatic” relaxation mechanism, while the similar time scales of the ground-state recovery and excited-state decay for TB are the hallmarks of the “adiabatic” relaxation mechanism.

for the equilibrium ground state were 2.5–3.8 eV for LGS, 3.0–4.0 eV for TB, and 2.5–2.9 eV for the experiments.

For both of the simulated hydrated electron models, Figure 4 shows that the *p*-state photoelectron spectroscopy peak decays in a time roughly equal to (but not precisely the same as, as

discussed below) the survival probability lifetime. The dynamics of the hot *s*-state, however are significantly different between the two models: the hot ground-state TB electron cools almost instantly (i.e., in a time the about the same as the decay of *p*-state that produces it) while the LGS electron shows a noticeably longer cooling process that much better resembles the experiments. Finally, the recovery of the equilibrium ground state represents a convolution of the radiationless transition kinetics and the subsequent ground-state cooling dynamics. The LGS noncavity ground-state recovery signal shows significantly slower dynamics than the excited-state decay, largely due to the slow ground-state cooling, which is consistent with the “nonadiabatic” relaxation picture and in agreement with experiment. For the TB cavity model, the ground-state recovery is only marginally slower than the excited-state decay, in contrast to experiment.

Given that our simulations appear to provide a fairly realistic description of the pump–probe photoelectron spectroscopy experiment, we turn next to the question of how accurately the experiment can determine the electron’s excited-state lifetime. One would expect that integration of the peak that corresponds to the *p*-like state would provide a good approximation to the instantaneous excited-state population, so that the time decay of the integrated peak would be a good measure of the excited-state lifetime. This expectation, however, only makes sense provided that the cross-section for ionization of the excited-state electron is approximately constant with time. Table 1 and the SI show that the cross sections for ionization of higher-lying excited states are larger than that of the lowest-lying *p*-like excited state. This is particularly important for the LGS model of the hydrated electron, because the fact that the LGS electron’s ground-state absorption is homogeneously broadened means that a significant fraction (~60%) of the excited electrons end up in states higher than the lowest *p*-like state (with 33% higher than the second *p*-like excited state; see SI). As the excited electron relaxes to the lowest of these excited states over the first few tens of fs, the occupied-state energy decreases, explaining the slight shift to lower kinetic energies of the excited-state peak (cf. Figure 1a). This early time relaxation is also accompanied by a significant decrease of the ionization transition dipole, which leads to an apparent decay of the excited-state TRPES peak that is independent of the excited-state population.

In Figure 5, we compare the integral of the TRPES excited-state peak (the same data as the blue dotted curves in Figure 4 but without convolution with instrumental response) to the actual calculated survival probability dynamics. For the TB cavity model, shown in panel b, the two decays are in reasonable agreement, but for the LGS noncavity model, shown in panel a, it is clear that the *p*-state TRPES peak decays faster than the actual underlying excited-state population. Given that multiple experiments have indicated that the absorption spectrum of the hydrated electron is homogeneously broadened,^{28–32} the data in Figure 5 strongly suggest that the actual excited-state lifetime of the hydrated electron is ~30% longer than the measured decay of the *p*-state photoelectron spectra peak. Thus, for the 60–75 fs photoelectron spectroscopy peak decay measured by experiment, the expected underlying lifetime of the hydrated electron should be ~100 fs.

Finally, we turn back to the fact that the TRPES experiments of Suzuki and co-workers were angle-resolved; these workers measured a significant anisotropy of the excited-state peak, verifying its origin as coming from a *p*-like excited state, and

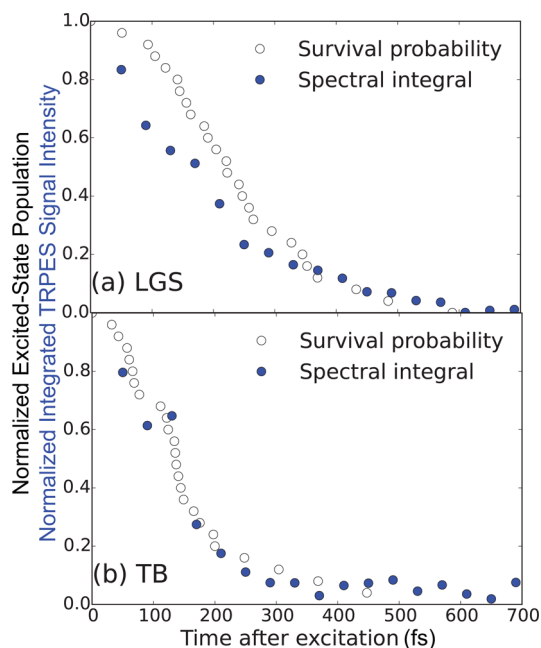


Figure 5. Excited-state survival probability (unfilled circles; see the SI) and decay of the integrated *p*-state photoelectron peak (blue circles, same data as in Figure 4 without convolution with the instrumental response) for the (a) LGS and (b) TB models of the hydrated electron. The fact that excitation of the homogeneously broadened LGS absorption spectrum leads to significant population of higher-lying excited states with larger photoionization cross sections causes the *p*-state photoelectron peak to decay faster than the underlying population. This suggests that the experimentally measured 60–75 fs decay time of this peak corresponds to an actual lifetime of ~100 fs.

saw that the anisotropy decayed in roughly 40 fs.⁴⁸ Although a full simulation of the angle-resolved TRPES experiment is beyond the scope of our computational capabilities, we did, however, examine the loss of orientation of the excited-state wave function, which should be directly connected the experimentally observed anisotropy decay. To do this, we constructed the moment-of-inertia tensor for the excited-state wave function, and monitored the reorientation of a unit vector, $\mathbf{d}(t)$, pointing in the direction of the largest principle moment as a function of time, averaged over our nonequilibrium ensembles. The results of this calculation for both the TB (green curve) and LGS (blue curve) hydrated electron models are shown in Figure 6.

Figure 6 makes clear that LGS noncavity electron shows significant depolarization during the first 40 fs, a result in good general agreement with experiment. In contrast, the TB cavity electron loses less than 10% of its initial orientation over this same time period, and thus is again inconsistent with the experimental observations. This difference in early time reorientational dynamics has its origins in the fact that the two models show absorption spectra with different underlying broadening mechanisms. Excitation of the homogeneously broadened LGS electron leads to nonadiabatic transitions in the excited-state manifold on an ~40 fs time scale, and since each nonadiabatic transition effectively changes the orientation of the excited *p*-like state by roughly 90°, orientational memory is lost on the time scale of this relaxation. In other words, the same physics that produce the early time red-shift of the LGS excited-state TRPES peak also cause the loss of its anisotropy. For the TB electron, on the other hand, excitation is

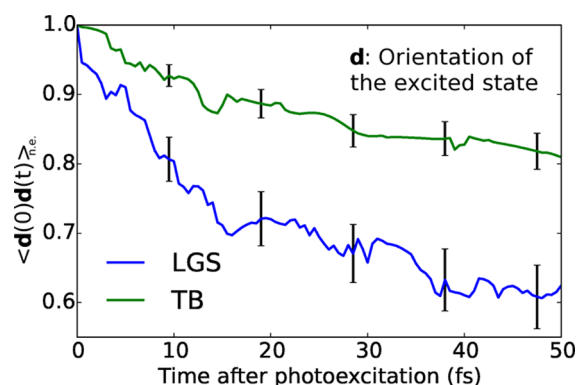


Figure 6. Orientational memory of the occupied excited-state following photoexcitation for the TB cavity (green curve) and LGS noncavity (blue curve) hydrated electron models. The orientation of the excited state is represented by a unit vector $\mathbf{d}(t)$ pointing along the excited-state wave function's principle moment of inertia. The LGS electron shows a rapid decay of the initial orientation due to rapid nonadiabatic transitions between electronic excited states with different average orientations, in agreement with the experimentally observed ~ 40 fs decay of the anisotropy of the excited-state TRPES peak.⁴⁸ The TB electron, in contrast, can reorient only by physical rotation of the excited-state cavity, and thus shows little early time loss in orientational memory, in contrast to experiment.

predominantly to the lowest excited state, where the only mechanism for loss of anisotropy is physical reorientation of the entire excited-state cavity. This reorientation is a slow, diffusion-based process, so that memory of the initial orientation persists for a long time (~ 1 ps).⁶⁸ Indeed, the fact that reorientation of a cavity electron's cavity is slow is the reason why such models predict inhomogeneously broadened absorption spectra, and as pointed out above, the predictions of polarized hole-burning for inhomogeneously broadened cavity hydrated electron models⁶⁸ have not been observed experimentally.^{28,29,31,32}

CONCLUSION

In this paper, we have worked to make a direct connection between the results of nonadiabatic mixed quantum/classical molecular dynamics simulations and time-resolved photoelectron spectroscopy experiments on the hydrated electron.^{46–48} We found that a cavity model of the hydrated electron (TB) showed excited-state relaxation dynamics reminiscent of the “adiabatic mechanism”, in which the excited-state lifetime is longer than the ground-state cooling time. The noncavity hydrated electron model (LGS), in contrast, showed dynamics that clearly fall into the “non-adiabatic mechanism”, with ground-state cooling that persists for times longer than the excited-state lifetime. The TRPES experiments are clearly more consistent with the noncavity model.

We also see two additional features of the predicted pump–probe photoelectron spectroscopy for the cavity hydrated electron model that are not in accord with experiment. First, the TB model shows a rapid solvent-induced increase of the occupied p -state energy of the excited electron, predicting a dynamic shift to higher kinetic energies (lower electron binding energies) at early times that is not seen in experiment. Second, the adiabatic relaxation mechanism shown by the TB model predicts essentially two-state kinetics in the pump–probe photoelectron spectroscopy with a large gap between the p - and

s -states. In contrast, the experiments show clear dynamical shift of the lower-kinetic-energy peak due to cooling of hot ground-state electrons as well as an early time shift of the p -state peak to lower energies, both of which are well-mirrored by the LGS model. The LGS model also predicts ground-state cooling dynamics on a nearly identical time scale as that seen in experiment.

The fact that there is a rapid loss in anisotropy of the p -state TRPES peak⁴⁸ can be explained by the same physics that causes the early time red-shift of this peak. The hydrated electron's absorption spectrum is homogeneously broadened, so that photoexcitation initially populates excited states above the lowest p -like excited state. Following excitation, a rapid series of nonadiabatic transitions among the electronic excited states decreases the average occupied state energy and causes a loss of orientational memory, features that are reasonably well represented by a noncavity picture. Cavity models that predict inhomogeneously broadened absorption spectra, in contrast, do not predict any significant early time loss in anisotropy because they require physical reorientation of the excited state that is too slow to act on the experimentally observed ~ 40 fs time scale.

Finally, the fact that the cross sections for photoionization are higher for higher-lying excited states means that the decay of the p -state peak in the transient photoelectron spectrum is somewhat faster than the underlying excited-state lifetime. By comparing the simulated photoelectron dynamics with the actual survival probability, we believe that the experimentally observed 60–75 fs decay of the p -state photoelectron peak corresponds to an underlying hydrated electron excited-state lifetime of ~ 100 fs. Overall, our work suggests that any good simulation model of the hydrated electron must follow the “nonadiabatic” relaxation mechanism and have a homogeneously broadened absorption spectrum to be consistent with the recent time-resolved photoelectron spectroscopy experiments.

ASSOCIATED CONTENT

Supporting Information

The Supporting Information is available free of charge on the ACS Publications website at DOI: 10.1021/acs.jpcc.6b07852.

Detailed description of nonequilibrium trajectories, exploration of decoherence of the two different models for the excited hydrated electron and how this should affect the calculated lifetime from surface hopping, calculation of time-resolved photoelectron spectra including cross sections, distribution of excited-states and their relative ionization cross sections leading to non-Condon effects, and surface plots of raw calculated TRPES signals (PDF)

AUTHOR INFORMATION

Corresponding Author

*E-mail: schwartz@chem.ucla.edu. Phone: 310-206-4113.

ORCID

Benjamin J. Schwartz: 0000-0003-3257-9152

Notes

The authors declare no competing financial interest.

ACKNOWLEDGMENTS

This work was supported by the National Science Foundation under Grant Number CHE-1565434. The authors thank Holly Williams and Dan Neumark for providing the experimental TRPES data from in ref 46 used in Figure 4c, and Shutaro Karashima and Toshinori Suzuki for providing the experimental TRPES data from ref 48 used in Figure 2c. We also thank all of the forementioned for a critical reading of an earlier draft of this manuscript. The authors also acknowledge helpful discussions with Prof. William J. Glover and Erik Farr.

REFERENCES

- (1) Garrett, B. C.; Dixon, D. A.; Camaioni, D. M.; Chipman, D. M.; Johnson, M. A.; Jonah, C. D.; Kimmel, G. A.; Miller, J. H.; Rescigno, T. N.; Rosicky, P. J.; et al. Role of water in electron-initiated processes and radical chemistry: Issues and scientific advances. *Chem. Rev.* **2005**, *105*, 355–390.
- (2) Gu, J.; Leszczynski, J.; Schaefer, H. F., III Interactions of electrons with bare and hydrated biomolecules: from nucleic acid bases to DNA segments. *Chem. Rev.* **2012**, *112*, 5603–5640.
- (3) Turi, L.; Rosicky, P. J. Theoretical studies of spectroscopy and dynamics of hydrated electrons. *Chem. Rev.* **2012**, *112*, 5641–5674.
- (4) Kumar, A.; Walker, J. A.; Bartels, D. M.; Sevilla, M. D. A simple *Ab Initio* Model for the Hydrated Electron that Matches Experiment. *J. Phys. Chem. A* **2015**, *119*, 9148.
- (5) Larsen, R. E.; Glover, W. J.; Schwartz, B. J. Does the Hydrated Electron Occupy a Cavity? *Science* **2010**, *329*, 65–69.
- (6) Jacobson, L. D.; Herbert, J. M. Comment on “Does the Hydrated Electron Occupy a Cavity?” *Science* **2011**, *331*, 1387–1387.
- (7) Turi, L.; Madarász, A. Comment on “Does the Hydrated Electron Occupy a Cavity?” *Science* **2011**, *331*, 1387–1387.
- (8) Larsen, R. E.; Glover, W. J.; Schwartz, B. J. Response to comments on “Does the hydrated electron occupy a cavity?” *Science* **2011**, *331*, 1387–1387.
- (9) Jacobson, L. D.; Herbert, J. M. A one-electron model for the aqueous electron that includes many-body electron-water polarization: Bulk equilibrium structure, vertical electron binding energy, and optical absorption spectrum. *J. Chem. Phys.* **2010**, *133*, 154506.
- (10) Herbert, J. M.; Jacobson, L. D. Structure of the Aqueous Electron: Assessment of One-Electron Pseudopotential Models in Comparison to Experimental Data and Time-Dependent Density Functional Theory. *J. Phys. Chem. A* **2011**, *115*, 14470–14483.
- (11) Turi, L. Hydrated Electrons in Water Clusters: Inside or Outside, Cavity or Noncavity? *J. Chem. Theory Comput.* **2015**, *11*, 1745–1755.
- (12) Turi, L. On the applicability of one-and many-electron quantum chemistry models for hydrated electron clusters. *J. Chem. Phys.* **2016**, *144*, 154311.
- (13) Glover, W. J.; Schwartz, B. J. Short-Range Electron Correlation Stabilizes Non-Cavity Solvation of the Hydrated Electron. *J. Chem. Theory Comput.* **2016**, *12*, 5117.
- (14) Kevan, L. Solvated electron structure in glassy matrixes. *Acc. Chem. Res.* **1981**, *14*, 138–145.
- (15) Zhan, C.-G.; Dixon, D. A. The nature and absolute hydration free energy of the solvated electron in water. *J. Phys. Chem. B* **2003**, *107*, 4403–4417.
- (16) Rosicky, P. J.; Schnitker, J. The hydrated electron: Quantum simulation of structure, spectroscopy, and dynamics. *J. Phys. Chem.* **1988**, *92*, 4277–4285.
- (17) Turi, L.; Borgis, D. Analytical investigations of an electron–water molecule pseudopotential. II. Development of a new pair potential and molecular dynamics simulations. *J. Chem. Phys.* **2002**, *117*, 6186–6195.
- (18) Casey, J. R.; Larsen, R. E.; Schwartz, B. J. Resonance Raman and temperature-dependent electronic absorption spectra of cavity and noncavity models of the hydrated electron. *Proc. Natl. Acad. Sci. U. S. A.* **2013**, *110*, 2712–7.
- (19) Casey, J. R.; Kahros, A.; Schwartz, B. J. To be or not to be in a cavity: the hydrated electron dilemma. *J. Phys. Chem. B* **2013**, *117*, 14173–14182.
- (20) Uhlig, F.; Marsalek, O.; Jungwirth, P. Unraveling the complex nature of the hydrated electron. *J. Phys. Chem. Lett.* **2012**, *3*, 3071–3075.
- (21) Glover, W. J.; Casey, J. R.; Schwartz, B. J. Free energies of quantum particles: The coupled-perturbed quantum umbrella sampling method. *J. Chem. Theory Comput.* **2014**, *10*, 4661–4671.
- (22) Casey, J. R.; Schwartz, B. J.; Glover, W. J. Free Energies of Cavity and Non-cavity Hydrated Electrons Near the Instantaneous Air/Water Interface. *J. Phys. Chem. Lett.* **2016**, *7*, 3192–8.
- (23) Borsarelli, C. D.; Bertolotti, S. G.; Previtali, C. M. Thermodynamic changes associated with the formation of the hydrated electron after photoionization of inorganic anions: a time-resolved photoacoustic study. *Photochem. Photobiol. Sci.* **2003**, *2*, 791–795.
- (24) Bratos, S.; Leicknam, J.-C.; Borgis, D.; Staib, A. Subpicosecond pump-probe absorption of the hydrated electron: Nonlinear response theory and computer simulation. *Phys. Rev. E: Stat. Phys., Plasmas, Fluids, Relat. Interdiscip. Top.* **1997**, *55*, 7217.
- (25) Shkrob, I. A. Pump–probe polarized transient hole burning (PTHB) dynamics of hydrated electron revisited. *Chem. Phys. Lett.* **2008**, *467*, 84–87.
- (26) Schwartz, B. J.; Rosicky, P. J. Pump–probe spectroscopy of the hydrated electron: A quantum molecular dynamics simulation. *J. Chem. Phys.* **1994**, *101*, 6917–6926.
- (27) Schwartz, B. J.; Rosicky, P. J. Hydrated electrons as a probe of local anisotropy: Simulations of ultrafast polarization-dependent spectral hole burning. *Phys. Rev. Lett.* **1994**, *72*, 3282.
- (28) Emde, M. F.; Baltuska, A.; Kummrow, A.; Pshenichnikov, M. S.; Wiersma, D. A. Ultrafast librational dynamics of the hydrated electron. *Phys. Rev. Lett.* **1998**, *80*, 4645.
- (29) Baltuska, A.; Emde, M. F.; Pshenichnikov, M. S.; Wiersma, D. A. Early-time dynamics of the photoexcited hydrated electron. *J. Phys. Chem. A* **1999**, *103*, 10065–10082.
- (30) Tauber, M. J.; Mathies, R. A. Resonance Raman spectra and vibronic analysis of the aqueous solvated electron. *Chem. Phys. Lett.* **2002**, *354*, 518–526.
- (31) Thaller, A.; Laenen, R.; Laubereau, A. Femtosecond spectroscopy of the hydrated electron: novel features in the infrared. *Chem. Phys. Lett.* **2004**, *398*, 459–465.
- (32) Cavanagh, M. C.; Martini, I. B.; Schwartz, B. J. Revisiting the pump–probe polarized transient hole-burning of the hydrated electron: Is its absorption spectrum inhomogeneously broadened? *Chem. Phys. Lett.* **2004**, *396*, 359–366.
- (33) Alfano, J. C.; Walhout, P.; Kimura, Y.; Barbara, P. F. Ultrafast transient-absorption spectroscopy of the aqueous solvated electron. *J. Chem. Phys.* **1993**, *98*, 5996.
- (34) Kimura, Y.; Alfano, J. C.; Walhout, P.; Barbara, P. F. Ultrafast Transient Absorption Spectroscopy of the Solvated Electron in Water. *J. Phys. Chem.* **1994**, *98*, 3450–8.
- (35) Silva, C.; Walhout, P. K.; Yokoyama, K.; Barbara, P. F. Femtosecond Solvation Dynamics of the Hydrated Electron. *Phys. Rev. Lett.* **1998**, *80*, 1086–1089.
- (36) Yokoyama, K.; Silva, C.; Son, D. H.; Walhout, P. K.; Barbara, P. F. Detailed Investigation of the Femtosecond Pump-Probe Spectroscopy of the Hydrated Electron. *J. Phys. Chem. A* **1998**, *102*, 6957–6966.
- (37) Assel, M.; Laenen, R.; Laubereau, A. Femtosecond solvation dynamics of solvated electrons in neat water. *Chem. Phys. Lett.* **2000**, *317*, 13–22.
- (38) Hertwig, A.; Hippler, H.; Unterreiner, A.-N. Temperature-dependent studies of solvated electrons in liquid water with two and three femtosecond pulse sequences. *Phys. Chem. Chem. Phys.* **2002**, *4*, 4412–4419.
- (39) Pshenichnikov, M. S.; Baltuska, A.; Wiersma, D. A. Hydrated-electron population dynamics. *Chem. Phys. Lett.* **2004**, *389*, 171–175.

- (40) Schwartz, B. J.; Rossky, P. J. Aqueous solvation dynamics with a quantum mechanical Solute: Computer simulation studies of the photoexcited hydrated electron. *J. Chem. Phys.* **1994**, *101*, 6902–6916.
- (41) Winter, B.; Faubel, M. Photoemission from liquid aqueous solutions. *Chem. Rev.* **2006**, *106*, 1176–1211.
- (42) Siefermann, K. R.; Liu, Y.; Lugovoy, E.; Link, O.; Faubel, M.; Buck, U.; Winter, B.; Abel, B. Binding energies, lifetimes and implications of bulk and interface solvated electrons in water. *Nat. Chem.* **2010**, *2*, 274–279.
- (43) Tang, Y.; Suzuki, Y.-i.; Shen, H.; Sekiguchi, K.; Kurahashi, N.; Nishizawa, K.; Zuo, P.; Suzuki, T. Time-resolved photoelectron spectroscopy of bulk liquids at ultra-low kinetic energy. *Chem. Phys. Lett.* **2010**, *494*, 111–116.
- (44) Shreve, A. T.; Yen, T. A.; Neumark, D. M. Photoelectron spectroscopy of hydrated electrons. *Chem. Phys. Lett.* **2010**, *493*, 216–219.
- (45) Lübcke, A.; Buchner, F.; Heine, N.; Hertel, I. V.; Schultz, T. Time-resolved photoelectron spectroscopy of solvated electrons in aqueous NaI solution. *Phys. Chem. Chem. Phys.* **2010**, *12*, 14629–14634.
- (46) Elkins, M. H.; Williams, H. L.; Shreve, A. T.; Neumark, D. M. Relaxation Mechanism of the Hydrated Electron. *Science* **2013**, *342*, 1496–1499.
- (47) Elkins, M. H.; Williams, H. L.; Neumark, D. M. Isotope effect on hydrated electron relaxation dynamics studied with time-resolved liquid jet photoelectron spectroscopy. *J. Chem. Phys.* **2016**, *144*, 184503.
- (48) Karashima, S.; Yamamoto, Y.-i.; Suzuki, T. Resolving Non-adiabatic Dynamics of Hydrated Electrons Using Ultrafast Photoemission Anisotropy. *Phys. Rev. Lett.* **2016**, *116*, 137601.
- (49) Bragg, A. E.; Verlet, J. R. R.; Kammrath, A.; Cheshnovsky, O.; Neumark, D. M. Hydrated electron dynamics: from clusters to bulk. *Science* **2004**, *306*, 669–71.
- (50) Coe, J. V.; Williams, S. M.; Bowen, K. H. Photoelectron spectra of hydrated electron clusters vs. cluster size: connecting to bulk. *Int. Rev. Phys. Chem.* **2008**, *27*, 27–51.
- (51) Ehrler, O. T.; Neumark, D. M. Dynamics of Electron Solvation in Molecular Clusters. *Acc. Chem. Res.* **2009**, *42*, 769.
- (52) Siefermann, K. R.; Abel, B. The hydrated electron: A seemingly familiar chemical and biological transient. *Angew. Chem., Int. Ed.* **2011**, *50*, 5264–5272.
- (53) Larsen, R. E.; Bedard-Hearn, M. J.; Schwartz, B. J. Exploring the role of decoherence in condensed-phase nonadiabatic dynamics: A comparison of different mixed quantum/classical simulation algorithms for the excited hydrated electron. *J. Phys. Chem. B* **2006**, *110*, 20055–20066.
- (54) Toukan, K.; Rahman, A. Molecular-dynamics study of atomic motions in water. *Phys. Rev. B: Condens. Matter Mater. Phys.* **1985**, *31*, 2643–2648.
- (55) Evans, D. J.; Holian, B. L. The nose–hoover thermostat. *J. Chem. Phys.* **1985**, *83*, 4069–4074.
- (56) Phillips, J. C.; Kleinman, L. New method for calculating wave functions in crystals and molecules. *Phys. Rev.* **1959**, *116*, 287–294.
- (57) Cohen, M. L.; Heine, V. Pseudopotential theory of cohesion and structure. *Solid State Phys.* **1970**, *24*, 37.
- (58) Szasz, L. *Pseudopotential theory of atoms and molecules*; John Wiley & Sons Inc.: New York, 1985.
- (59) Tully, J. C. Molecular dynamics with electronic transitions. *J. Chem. Phys.* **1990**, *93*, 1061–1071.
- (60) Tully, J. Mixed quantum–classical dynamics. *Faraday Discuss.* **1998**, *110*, 407–419.
- (61) Schwartz, B. J.; Bittner, E. R.; Prezhdo, O. V.; Rossky, P. J. Quantum decoherence and the isotope effect in condensed phase nonadiabatic molecular dynamics simulations. *J. Chem. Phys.* **1996**, *104*, 5942–5955.
- (62) Prezhdo, O. V.; Rossky, P. J. Evaluation of quantum transition rates from quantum-classical molecular dynamics simulations. *J. Chem. Phys.* **1997**, *107*, 5863–5878.
- (63) Prezhdo, O. V.; Rossky, P. J. Relationship between quantum decoherence times and solvation dynamics in condensed phase chemical systems. *Phys. Rev. Lett.* **1998**, *81*, 5294.
- (64) Bedard-Hearn, M. J.; Larsen, R. E.; Schwartz, B. J. Mean-field dynamics with stochastic decoherence (MF-SD): A new algorithm for nonadiabatic mixed quantum/classical molecular-dynamics simulations with nuclear-induced decoherence. *J. Chem. Phys.* **2005**, *123*, 234106.
- (65) Borgis, D.; Rossky, P. J.; Turi, L. Nuclear quantum effects on the nonadiabatic decay mechanism of an excited hydrated electron. *J. Chem. Phys.* **2007**, *127*, 174508.
- (66) Prezhdo, O. V.; Rossky, P. J. Solvent mode participation in the nonradiative relaxation of the hydrated electron. *J. Phys. Chem.* **1996**, *100*, 17094–17102.
- (67) Bedard-Hearn, M. J.; Larsen, R. E.; Schwartz, B. J. Projections of Quantum Observables onto Classical Degrees of Freedom in Mixed Quantum/Classical Simulations: Understanding Linear Response Failure for the Photoexcited Hydrated Electron. *Phys. Rev. Lett.* **2006**, *97*, 130403.
- (68) Schwartz, B. J.; Rossky, P. J. Hydrated Electrons as a Probe of Local Anisotropy: Simulations of Ultrafast Polarization-Dependent Spectral Hole-Burning. *Phys. Rev. Lett.* **1994**, *72*, 3282–5.